

# Not Only Hypoxia- but Radiation-Induced Epithelial-Mesenchymal Transition Is Modulated by Hypoxia-Inducible Factor 1 in A549 Lung Cancer Cells

(epithelial-mesenchymal transition / HIF-1 $\alpha$  / HIF-1 $\alpha$  inhibitor / JNK / E-cadherin / vimentin)

M. SATO<sup>1,2,3</sup>, K. HIROSE<sup>1,2,3</sup>, K. ICHISE<sup>1</sup>, H. YOSHINO<sup>4</sup>, T. HARADA<sup>2</sup>,  
Y. HATAYAMA<sup>1</sup>, H. KAWAGUCHI<sup>1</sup>, M. TANAKA<sup>1</sup>, I. FUJIOKA<sup>1</sup>, Y. TAKAI<sup>2,3</sup>,  
M. AOKI<sup>1</sup>

<sup>1</sup>Department of Radiation Oncology, Hirosaki University Graduate School of Medicine, 5 Zaifu-cho, Hirosaki, Japan

<sup>2</sup>Southern Tohoku BNCT Research Center, Yatsuyamada, Koriyama, Japan

<sup>3</sup>Department of Radiation Oncology, Southern Tohoku General Hospital, Yatsuyamada, Koriyama, Japan

<sup>4</sup>Department of Radiation Science, Hirosaki University Graduate School of Health Sciences, Hon-cho, Hirosaki, Japan

**Abstract.** Hypoxia leads to post-treatment metastasis and recurrences of cancer via the epithelial-mesenchymal transition (EMT). Radiotherapy itself may also contribute to the acquisition of EMT phenotypes. Despite extensive studies on the EMT driven by either hypoxia or radiation stimuli, the molecular mechanisms characterizing these EMT events remain unclear. Thus, we aimed to evaluate the differences in the molecular pathways between hypoxia-induced EMT (Hypo-EMT) and radiation-induced EMT (R-EMT). Further, we investigated the therapeutic effects of HIF-1 $\alpha$  inhibitor (LW6) on Hypo-EMT and R-EMT cells. A549 cells, lung adenocarcinoma cell line, acquired enhanced wound-healing activity under both hypoxia and irradiation. Localization of E-cadherin was altered from the cell membrane to

the cytoplasm in both hypoxia and irradiated conditions. Of note, the expression levels of vimentin, one of the major EMT markers, was enhanced in irradiated cells, while it decreased under hypoxia condition. Importantly, LW6 significantly blocked EMT-related malignant phenotypes in both Hypo-EMT cells and R-EMT cells with concomitant re-location of E-cadherin onto the cell membrane. Moreover, LW6 deflected stress responsive signalling, JNK, activated sustainably under hypoxic condition, and the blockage of JNK impaired EMT phenotypes. Together, this work demonstrated the molecular events underlying Hypo-EMT and R-EMT, and highlighted HIF-1 $\alpha$  as a therapeutic target not only in Hypo-EMT, but also in R-EMT.

## Introduction

Hypoxic conditions are known to be closely associated with cancer metastasis and recurrence (El Guerrab et al., 2017; Zhang et al., 2017). Moreover, the surviving cells that have developed radioresistance reportedly acquire cell migratory and invasive capabilities through the epithelial-mesenchymal transition (EMT) induced by radiation in glioblastoma cells (Zhai et al., 2006).

Recent reports suggest that radiotherapy further promotes the cell migratory and invasive potential of cancer cells in which the EMT has occurred, and this may lead to a vicious cycle. The local control rate after stereotactic body radiotherapy (SBRT) for oligometastatic lung tumours from colorectal cancer was significantly worse than that of oligometastatic lung tumours from other primitive tumours (Takeda et al., 2011). Moreover, the study also showed that local recurrence might occur

---

Received October 9, 2020. Accepted June 20, 2021.

This work was supported by JSPS KAKENHI, Grant-in-Aid for Young Scientists (B; 15K19764).

Corresponding author: Katsumi Hirose, Department of Radiation Oncology, Southern Tohoku BNCT Research Center, 7-10 Yatsuyamada, Koriyama, Fukushima 963-8052, Japan. Phone & Fax: (+81) 24-934-5322; e-mail: khirose@hirosaki-u.ac.jp

Abbreviations: EMT – epithelial-mesenchymal transition, ERK – extracellular signal-regulated kinase, HIF-1 $\alpha$  – hypoxia-inducible factor 1 $\alpha$ , Hypo-EMT – hypoxia-induced EMT, JNK – c-Jun N-terminal kinase, MAPK – mitogen-activated protein kinase, p-JNK – phosphorylated c-Jun N-terminal kinase, pVHL – protein product of von Hippel-Lindau, R-EMT – radiation-induced EMT, SBRT – stereotactic body radiotherapy, VHL – von Hippel-Lindau.

even in cases with a negative margin after the resection of pulmonary or hepatic colorectal metastases. In contrast, the invasive spread around the main tumour and the number of satellite lesions are reportedly associated with the local or surgical margin recurrence rate (Nuzzo et al., 2008). Recently, Appelt et al. (2014) showed a trend toward worse locoregional control in patients treated with preoperative external chemoradiotherapy with 50.4 Gy in 28 fractions followed by a brachytherapy boost with 10 Gy in two fractions than in those treated with external chemoradiotherapy alone.

The induction of EMT is suggested to occur through hypoxia-inducible factor 1 $\alpha$  (HIF-1 $\alpha$ ), which is accumulated under the hypoxic environment formed in necrotic marginal areas of the tumour and upregulates EMT-related proteins such as Twist and Snail, enhancing metastasis and invasiveness (Cho et al., 2015). Therefore, suppression of the mechanisms that are promoted by radiotherapy appears to be a new strategy.

Thus far, no report has compared the mechanisms of hypoxia-induced EMT (Hypo-EMT) and radiation-induced EMT (R-EMT); moreover, evidence showing differences and similarities remains unclear. If there is a common universal stream for both the mechanisms, a blockade of this pathway may enhance the efficacy of radiotherapy, which is limited by hypoxic radioresistant cells. In this study, we aimed to evaluate the differences in the molecular pathways between Hypo-EMT and R-EMT and to elucidate the effectiveness of pathway-blocking agents, such as HIF-1 $\alpha$  inhibitors, depending on the induction type.

## Material and Methods

### Materials

Dulbecco's modified Eagle's medium (DMEM) was obtained from Sigma-Aldrich (St. Louis, MO). Penicillin and streptomycin were obtained from Gibco-Invitrogen Corp (Grand Island, NY). Foetal bovine serum (FBS) was obtained from PAA (Pasching, Austria). LW6 was purchased from Merck (Darmstadt, Germany), and c-Jun N-terminal kinase (JNK) inhibitor SP600125 was purchased from Wako (Osaka, Japan). LW6 and SP600125 were diluted in dimethyl sulphoxide (DMSO). Rabbit monoclonal antibodies against E-cadherin (#3195), N-cadherin (#4061), vimentin (#5741), JNK (#9258), phosphorylated JNK (p-JNK) (#4668) were purchased from Cell Signaling Technology (Beverly, MA). Goat polyclonal anti-actin antibody (C-11, sc-1615), HRP-conjugated anti-rabbit IgG (sc-2313), and HRP-conjugated anti-goat IgG (sc-2056) were obtained from Santa Cruz Biotechnology (Santa Cruz, CA). FITC-conjugated anti-E-cadherin antibody (612131) and mouse anti-human HIF-1 $\alpha$  antibody (610959) were purchased from BD Biosciences (San Jose, CA), and DAPI (H-1200) was obtained from Vector Laboratories (Burlingame, CA).

### Cell culture and growth conditions

Human lung adenocarcinoma cell line A549 was obtained from the RIKEN BRC Cell Bank (Kovadai, Tsukuba, Ibaraki, Japan). Cells were grown in DMEM supplemented with penicillin, streptomycin, and 10% heat-inactivated FBS at 37 °C under a humidified atmosphere containing 5% CO<sub>2</sub>. Hypoxia was defined as 1% oxygen. This environment was achieved by culturing cells in modular incubator chambers (Billups-Rothenberg, Del Mar, CA), which were flushed with gas mixtures (95% nitrogen/5% carbon dioxide) and sealed to maintain hypoxia after checking oxygen concentrations using an oxygen monitor (JKO-02 Ver.III; JIKCO, Tokyo, Japan).

### Irradiation

Cells were exposed to radiation (150 kVp, 5 mA; 0.5-mm Al filter) using an X-ray generator (MBR-1505R2; Hitachi Medial Co., Tokyo, Japan). Radiation doses of 0 to 10 Gy were administered at a dose-rate of approximately 1 Gy/min at room temperature.

### Wound-healing assay

The cells were seeded in a 35-mm dish (Iwaki Cell Biology, Japan) and incubated for 12 h under normoxia. Subsequently, the cells were pre-treated with DMSO, 20  $\mu$ M LW6 for 2 h. The cells were irradiated with 0 or 10 Gy after incubation under normoxia or hypoxia for 6 h and scratched just after irradiation. A 200- $\mu$ l pipette tip was used to draw three straight lines in each well, and the medium was abandoned. Cells were rinsed gently once with PBS and incubated under normoxia. Images were taken at the same point of the wounding area at 0 h and 24 h after the scratch. The data are presented as mean  $\pm$  standard error of mean (SE) values. The experiment was repeated three times independently.

### Invasion assay

An invasion assay was conducted using Coster Transwell 24-well plates with an 8.0- $\mu$ m polycarbonate membrane (Corning, Corning, NY). Cells irradiated with 0 or 10 Gy were seeded into each well of the Matrigel pre-coated upper chambers and treated with DMSO, 20  $\mu$ M LW6 or 5  $\mu$ M SP600125. The lower chambers were filled with FBS-free medium and the cells were incubated under normoxia or hypoxia. After 24 h, the non-invading cells were removed from the upper surface of the membrane with a swab stick. The invading cells were fixed with methanol, stained with 0.5% crystal violet, and counted in five random 100 $\times$  power fields under a microscope. The data are presented as mean  $\pm$  SE values. The experiment was repeated three times independently.

### Immunofluorescence microscopy

A cover glass was placed in each 35-mm dish (Iwaki), and the cells were seeded in the dishes for 12 h. Thereafter, the cells were pre-treated with DMSO, 20  $\mu$ M

LW6 for 2 h and exposed to hypoxia or 10 Gy irradiation. After 24 h, the cells were fixed with 4% paraformaldehyde, permeabilized with Triton X-100, and gently rinsed three times with PBS. The cells were then stained with FITC-conjugated anti-E-cadherin antibody (1 : 100) and DAPI. The cells were seeded in chamber slides (Matsunami, Osaka, Japan) and treated with DMSO, 20  $\mu$ M LW6 or 5  $\mu$ M SP600125 for 2 h. Fluorescent images were taken using a BIOREVO BZ-9000 fluorescence microscope (KEYENCE, Osaka, Japan).

### Western blot analysis

The cells were pre-treated with DMSO, 20  $\mu$ M LW6 for 2 h and exposed to hypoxia or 10 Gy irradiation. After 6 h, the cells were lysed and Western blot analysis was performed as described previously (Sato et al., 2015) with some modifications. The PVDF membranes were incubated with 4% Block Ace solution (DS Pharma

Biomedical, Osaka, Japan) overnight and incubated with corresponding primary antibody diluted to 1 : 1000 in Can Get Signal™ solution 1 (TOYOBO, Tokyo, Japan) for 1 h. After washing and incubation with secondary antibody diluted to 1 : 10,000 in Can Get Signal™ solution 2, the protein bands were visualized using enhanced chemiluminescence reagents (GE Healthcare UK Ltd, Buckinghamshire, UK). Images were acquired using a ChemiDoc™ XRS plus system and analysed with ImageLab™ (Bio-Rad). The protein expression levels were quantified using the imageJ software (version 1.53a) (National Institutes of Health, Bethesda, USA).

### Statistical analyses

The significance of differences was determined using the two-sided Student's *t*-test and Welch's *t*-test depending on data distribution. The significance level was set

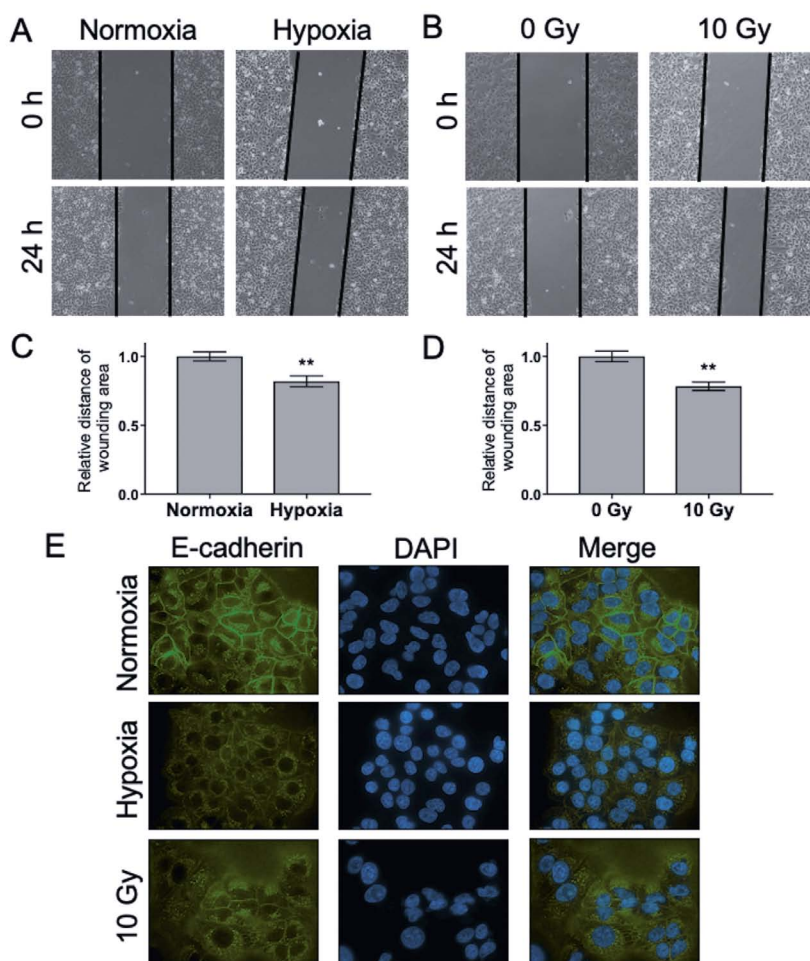


*Fig. 1.* Hypoxia and irradiation both increase wound-healing activity.

(A to D) Effects of hypoxia and irradiation in the wound-healing assay. (A) Cells were incubated under normoxia or hypoxia. (B) Cells were incubated under normoxia and irradiated with 10 Gy. (C and D) The relative distance of the wounding area at 24 h after the scratch. The distance of the wounding at 24 h was normalized by the wound at 0 h at the same point. The pictures were taken using a 100 $\times$  power field. (E) E-cadherin displacement was determined with immunofluorescence. The pictures were taken using a 1000 $\times$  power field.

at  $P < 0.05$ . Statistically significant differences are indicated as \*\*\*  $P < 0.001$ , \*\*  $P < 0.01$ , \*  $P < 0.05$ . The GraphPad Prism 7 software (GraphPad Software Inc., La Jolla, CA) was used for statistical analyses.

## Results

### *Hypoxia and irradiation both increased the wound-healing activity in A549 cells*

The EMT activity was evaluated with the wound-healing assay. Both 1% hypoxia and X-irradiation with 10 Gy accelerated the wound-healing activity in A549 cells (Fig. 1A-D). E-cadherin is known to play a role in cell adhesion and intercellular cell communication. The decrease in E-cadherin expression on the cell membrane induces acquisition of the EMT potential. Both hypoxia and irradiation partially displaced E-cadherin to the cy-

toplasm (Fig. 1E). These results suggest that the surviving irradiated cells acquire the potential of EMT via hypoxia as well as irradiation through different effects on the expression and displacement of E-cadherin.

### *HIF-1 $\alpha$ inhibitor suppressed vimentin expression induced by irradiation and altered the distribution of E-cadherin*

Our previous study confirmed the absence of cytotoxicity at different concentrations of LW6 up to 50  $\mu$ M in A549 cells and the potential of HIF-1 $\alpha$  inhibition (Sato et al., 2015). In EMT progression, vimentin and repression of E-cadherin are believed to be EMT markers. In the present study, hypoxia had a decreasing effect on the expression of vimentin (Fig. 2A). However, vimentin expression was enhanced by X-irradiation with 10 Gy (Fig. 2B). Treatment with LW6 resulted in considerable

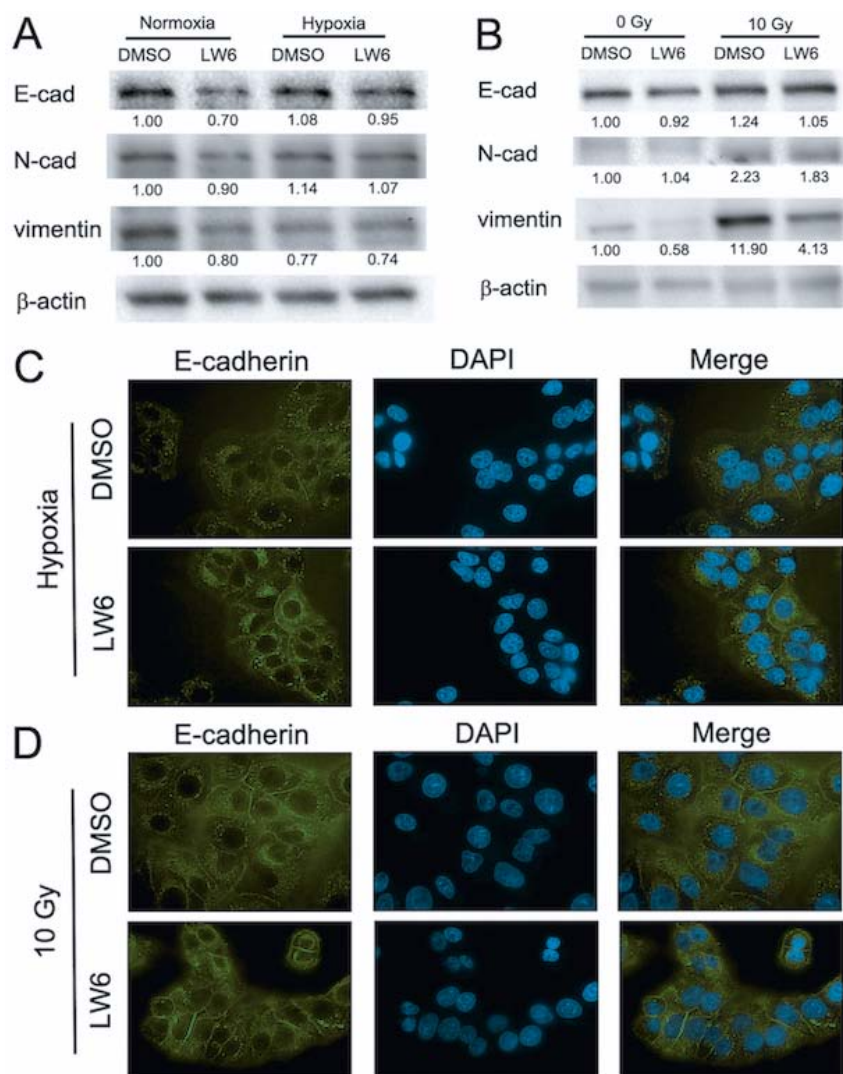


Fig. 2. HIF-1 inhibitor suppresses vimentin expression induced by irradiation and changes the distribution of E-cadherin. (A and B) EMT marker expression was detected by Western blot analysis. The numbers represent the relative protein expression levels/actin expression levels. (C and D) Alterations of E-cadherin localization. Cells were pre-treated with LW6 and exposed to hypoxia or 10 Gy irradiation. The pictures were taken using a 1000 $\times$  power field.

reduction of vimentin expression induced by irradiation (Fig. 2B). Although LW6 did not change the E-cadherin expression (Fig. 2A), the E-cadherin displacement onto the cell membrane appeared to increase after LW6 treatment in hypoxic conditions (Fig. 2C). These results suggest that LW6 can inhibit the Hypo-EMT and R-EMT progression via changes in E-cadherin localization and inhibition of vimentin over-expression at differing levels. Next, we investigated the inhibitory ability of LW6, a HIF-1 $\alpha$  inhibitor, on EMT. LW6 inhibited both Hypo-EMT and R-EMT in the invasion assay and wound healing assay (Fig. 3A-D). Cell migration and cell invasion are affected by cell proliferation; thus, we performed the trypan blue dye viability assay. LW6 did not significantly suppress cell proliferation in both hypoxic and irradiated cells (data not shown).

### *Prevention of JNK phosphorylation by HIF-1 $\alpha$ inhibitors delays wound healing in hypoxic conditions*

Recent studies suggest that in cultured cells under hypoxic conditions, signalling cascades through the MAPK

pathway are involved in the specific adaptation to the state of hypoxia (Poomthavorn et al., 2009). We examined the effects of hypoxia and irradiation on the expression of extracellular signal-regulated kinase (ERK)1/2, p38, JNK, and these phosphorylated proteins were examined. Hypoxia significantly increased the expression of p-JNK (Fig. 4A), and the expression of the others was modulated to degrees moderately differing from each other (data not shown). The JNK signalling pathway is reported to be involved in EMT progression (Desai et al., 2013; Cai et al., 2017); therefore, we investigated whether LW6 contributes to the modulation of JNK signalling. The phosphorylation of JNK induced by hypoxia was inhibited by LW6, and the wound-healing activity was decreased in correlation to p-JNK expression (Fig 4A and 3A). SP600125, as a JNK-specific inhibitor, also attenuated the wound-healing activity (Fig. 4C). These results suggest that LW6 has the ability to suppress JNK signalling that contributes to the activation of Hypo-EMT. However, in the irradiated cells, phosphorylation of JNK was unchanged in the experimental conditions (Fig. 4B). Nevertheless, the inhibition of the JNK pathway with SP600125 modulated irradiation-in-

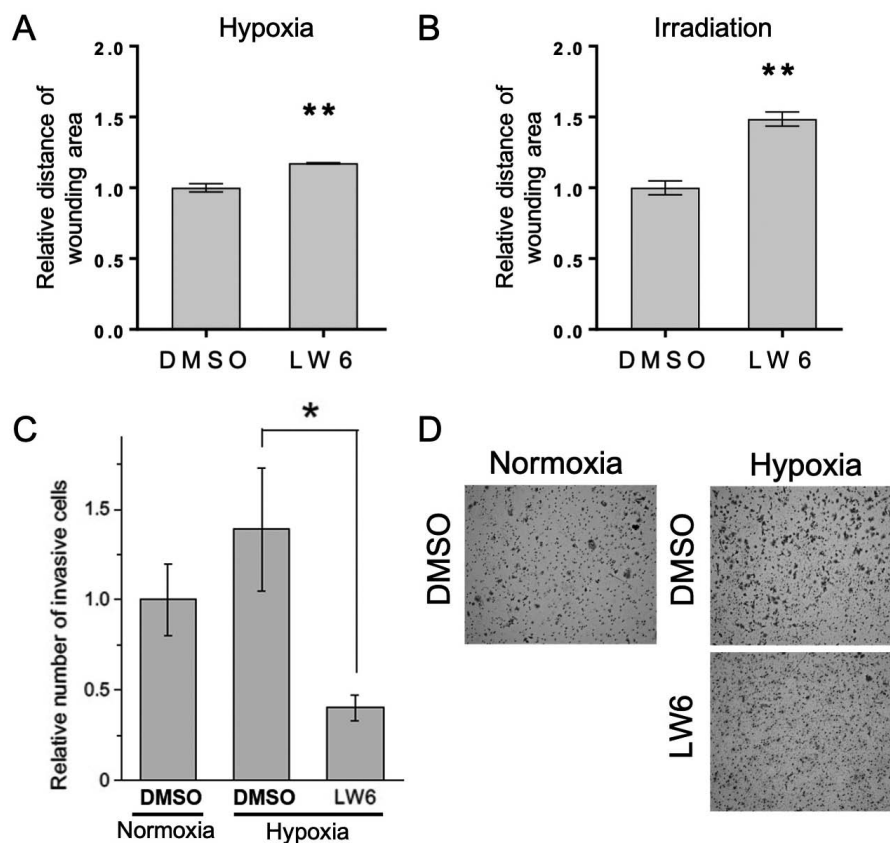


**Fig. 3.** HIF-1 inhibitor suppressed both Hypo-EMT and R-EMT.

Effects of LW6 on wound healing in (A) hypoxic cells and (B) irradiated cells. Cells were pre-treated with 20  $\mu$ M LW6, incubated under hypoxia, then re-oxygenated and scratched. Alternatively, the cells were irradiated with 10 Gy and scratched just after irradiation. After 24 h, the distance of the wounding area was measured. (C and D) Effect of LW6 in the invasion assay. Cells were seeded in the upper chamber with 20  $\mu$ M LW6 and incubated under normoxia or hypoxia. After 24 h, the invading cells at the lower surface of the membrane were counted. The pictures were taken using a 40 $\times$  power field.

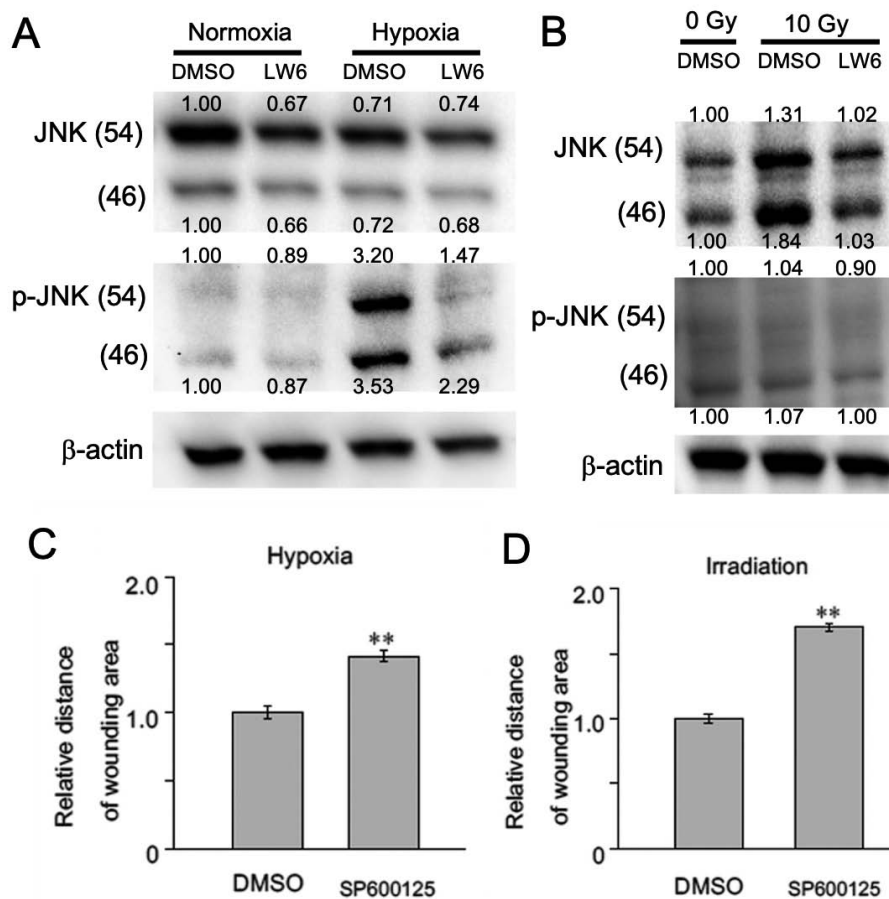


Fig. 4. HIF-1 inhibitor prevents phosphorylation of JNK and delays wound healing under hypoxia.

(A) Effects of LW6 on JNK and p-JNK expression in hypoxic cells. (B) Effect of LW6 on JNK and p-JNK expression in irradiated cells. The numbers represent the relative protein expression levels/actin expression levels. Effects of SP600125 on wound healing in (C) hypoxic cells and (D) irradiated cells.

duced wound-healing activation, similarly as under hypoxia (Fig. 4D). The phosphorylation of JNK induced by X-irradiation is reported to reach its peak level within 15 to 30 min of irradiation, and then it rapidly decreases and disappears (Yoshino et al., 2017). Therefore, based on the fact that SP600125 administration, which inhibits the phosphorylation of c-Jun by activated JNK-1, 2, and 3, decreased the expression level of JNK that was increased with 10 Gy irradiation, it was speculated that this agent might inhibit some positive feedback of JNK expression via the JNK pathway. The inhibition of the expression of JNK induced by irradiation was also observed with the administration of LW6 (Fig. 4B); therefore, LW6 might have an impact on the JNK pathway.

## Discussion

To our knowledge, this is the first study that shows the similarities and differences between Hypo-EMT and R-EMT. Importantly, LW6 significantly blocked EMT-related malignant phenotypes in both Hypo-EMT cells

and R-EMT cells with concomitant re-location of E-cadherin onto the cell membrane. The findings of these EMTs are summarized in Fig. 5 and Table 1. The displacement of E-cadherin into the cytoplasm was the main change related to EMT. The expression of vimentin was decreased by hypoxia in this study, although many re-

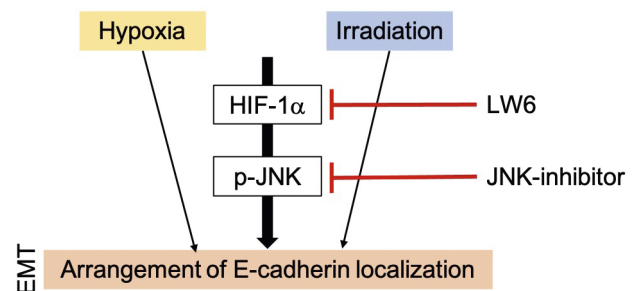


Fig. 5. LW6 blocks EMT-related malignant phenotypes in both Hypo-EMT cells and R-EMT cells with concomitant re-location of E-cadherin onto the cell membrane.

Table 1. Similarities and differences between Hypo-EMT and R-EMT

Findings	Hypo-EMT	R-EMT
Localization of E-cadherin	Cytoplasm	Cytoplasm
Vimentin expression level	No change	Up-regulated
Phosphorylation of JNK	Detected	Not detected

ports show that the vimentin expression is increased by hypoxia. According to Kang et al. (2019), the vimentin expression levels differed according to the length of exposure to hypoxia in some lung cancer cell lines. Moreover, the over-expression of vimentin was a prominent change related to EMT induction by irradiation.

In the tumour tissue, HIF-1 $\alpha$ , which is accumulated when the cells become hypoxic due to rapid growth and increased tumour oxygen consumption, enables adjustment to the hypoxic state via promoting expression of the genes related to tumour angiogenesis, invasion, and DNA repair (Carmeliet et al., 1998). HIF-1 $\alpha$  accumulation promotes tumour invasiveness in the cells, which is affected by repression of E-cadherin depending on NF- $\kappa$ B (Cheng et al., 2011). Furthermore, the PI3 kinase/Akt/HIF-1 $\alpha$  and JNK-mediated pathways are suggested to be involved in EMT induction (An et al., 2013). In breast cancer cells, secretion of TGF- $\beta$ 1 from mesenchymal stem cells induced by hypoxia leads to tumour progression (Hung et al., 2013). Therefore, the loss of the invasive potential of cancers, such as lower cell infiltration and cell migration, may be induced by depletion of HIF-1 $\alpha$ .

For R-EMT, there are several reports of differences from the Hypo-EMT. In normal cells, X-irradiation of 2 Gy predisposes to EMT induced by TGF- $\beta$  (Andarawewa et al., 2007), and ERK/GSK3/Snail signalling mediates EMT induction in alveolar cells (Nagarajan et al., 2012). In cancer cells, a few reports have shown that X-irradiation promotes over-expression of vimentin via TGF- $\beta$ , resulting in EMT (Zhou et al., 2011). However, whether HIF-1 $\alpha$  accumulation, previously reported to be induced by X-irradiation in a few studies (Singh-Gupta et al., 2009; Harada et al., 2012), influences EMT induction remains unknown.

In this study, it appeared that both stimuli for EMT induction were mediated through the activation of the JNK pathway, although there are some elemental differences in EMT expression under the two types of conditions. Moreover, LW6 deflected stress responsive signalling, JNK, activated sustainably under hypoxic condition, and the blockage of JNK impaired EMT phenotypes. Depletion of the protein product of VHL (pVHL) reportedly enhances phosphorylation of JNK, HIF-1 $\alpha$  independent (An et al., 2013). Therefore, considering that LW6 is potentially effective under both types of conditions, and that hypoxia and irradiation conditioning will occur simultaneously in the surviving

cells in actual radiotherapy, it appears that HIF-1 $\alpha$  inhibitors possess a larger potential in combination with irradiation than previously thought.

This work demonstrated the molecular events underlying Hypo-EMT and R-EMT, and highlighted HIF-1 $\alpha$  as a therapeutic target not only in Hypo-EMT, but also in R-EMT.

## References

- An, J., Liu, H., Magyar, C. E., Guo, Y., Veena, M. S., Srivatsan, E. S., Huang, J., Rettig, M. B. (2013) Hyperactivated JNK is a therapeutic target in pVHL-deficient renal cell carcinoma. *Cancer Res.* **73**, 1374-1385.
- Andarawewa, K. L., Erickson, A. C., Chou, W. S., Costes, S. V., Gascard, P., Mott, J. D., Bissell, M. J., Barcellos-Hoff, M. H. (2007) Ionizing radiation predisposes nonmalignant human mammary epithelial cells to undergo transforming growth factor  $\beta$  induced epithelial to mesenchymal transition. *Cancer Res.* **67**, 8662-8670.
- Appelt, A. L., Vogelius, I. R., Ploen, J., Rafaelsen, S. R., Lindebjerg, J., Havelund, B. M., Bentzen, S. M., Jakobsen, A. (2014) Long-term results of a randomized trial in locally advanced rectal cancer: no benefit from adding a brachytherapy boost. *Int. J. Radiat. Oncol. Biol. Phys.* **90**, 110-118.
- Cai, J., Du, S., Wang, H., Xin, B., Wang, J., Shen, W., Wei, W., Guo, Z., Shen, X. (2017) Tenascin-C induces migration and invasion through JNK/c-Jun signalling in pancreatic cancer. *Oncotarget* **8**, 74406-74422.
- Carmeliet, P., Dor, Y., Herbert, J. M., Fukumura, D., Brusselmans, K., Dewerchin, M., Neeman, M., Bono, F., Abramovitch, R., Maxwell, P., Koch, C. J., Ratcliffe, P., Moons, L., Jain, R. K., Collen, D., Keshert, E. (1998) Role of HIF-1 $\alpha$  in hypoxia-mediated apoptosis, cell proliferation and tumour angiogenesis. *Nature* **394**, 485-490.
- Cheng, Z. X., Sun, B., Wang, S. J., Gao, Y., Zhang, Y. M., Zhou, H. X., Jia, G., Wang, Y. W., Kong, R., Pan, S. H., Xue, D. B., Jiang, H. C., Bai, X. W. (2011) Nuclear factor- $\kappa$ B-dependent epithelial to mesenchymal transition induced by HIF-1 $\alpha$  activation in pancreatic cancer cells under hypoxic conditions. *PLoS One* **6**, e23752.
- Cho, K. H., Yu, S. L., Cho, D. Y., Park, C. G., Lee, H. Y. (2015) Breast cancer metastasis suppressor 1 (BRMS1) attenuates TGF- $\beta$ 1-induced breast cancer cell aggressiveness through downregulating HIF-1 $\alpha$  expression. *BMC Cancer* **15**, 829.
- Desai, S., Laskar, S., Pandey, B. N. (2013) Autocrine IL-8 and VEGF mediate epithelial-mesenchymal transition and invasiveness via p38/JNK-ATF-2 signalling in A549 lung cancer cells. *Cell Signal.* **25**, 1780-1791.
- El Guerrab, A., Cayre, A., Kwiatkowski, F., Privat, M., Rossignol, J. M., Rossignol, F., Penault-Llorca, F., Bignon, Y. J. (2017) Quantification of hypoxia-related gene expression as a potential approach for clinical outcome prediction in breast cancer. *PLoS One* **12**, e0175960.
- Harada, H., Inoue, M., Itasaka, S., Hirota, K., Morinibu, A., Shinomiya, K., Zeng, L., Ou, G., Zhu, Y., Yoshimura, M., McKenna, W. G., Muschel, R. J., Hiraoka, M. (2012) Cancer cells that survive radiation therapy acquire HIF-1 activ-

- ity and translocate towards tumour blood vessels. *Nat. Commun.* **3**, 783.
- Hung, S. P., Yang, M. H., Tseng, K. F., Lee, O. K. (2013) Hypoxia-induced secretion of TGF- $\beta$ 1 in mesenchymal stem cell promotes breast cancer cell progression. *Cell Transplant.* **22**, 1869-1882.
- Kang, N., Choi, S. Y., Kim, B. N., Yeo, C. D., Park, C. K., Kim, Y. K., Kim, T. J., Lee, S. B., Lee, S. H., Park, J. Y., Park, M. S., Yim, H. W., Kim, S. J. (2019) Hypoxia-induced cancer stemness acquisition is associated with CXCR4 activation by its aberrant promoter demethylation. *BMC Cancer* **19**, 148.
- Nagarajan, D., Melo, T., Deng, Z., Almeida, C., Zhao, W. (2012) ERK/GSK3 $\beta$ /Snail signaling mediates radiation-induced alveolar epithelial-to-mesenchymal transition. *Free Radic. Biol. Med.* **52**, 983-992.
- Nuzzo, G., Giuliani, F., Ardito, F., Vellone, M., Giovannini, I., Federico, B., Vecchio, F. M. (2008) Influence of surgical margin on type of recurrence after liver resection for colorectal metastases: a single-center experience. *Surgery* **143**, 384-393.
- Poomthavorn, P., Wong, S. H., Higgins, S., Werther, G. A., Russo, V. C. (2009) Activation of a prometastatic gene expression program in hypoxic neuroblastoma cells. *Endocr. Relat. Cancer* **16**, 991-1004.
- Sato, M., Hirose, K., Kashiwakura, I., Aoki, M., Kawaguchi, H., Hatayama, Y., Akimoto, H., Narita, Y., Takai, Y. (2015) LW6, a hypoxia-inducible factor 1 inhibitor, selectively induces apoptosis in hypoxic cells through depolarization of mitochondria in A549 human lung cancer cells. *Mol. Med. Rep.* **12**, 3462-3468.
- Singh-Gupta, V., Zhang, H., Banerjee, S., Kong, D., Raffoul, J. J., Sarkar, F. H., Hillman, G. G. (2009) Radiation-induced HIF-1 $\alpha$  cell survival pathway is inhibited by soy isoflavones in prostate cancer cells. *Int. J. Cancer* **124**, 1675-1684.
- Takeda, A., Kunieda, E., Ohashi, T., Aoki, Y., Koike, N., Takeda, T. (2011) Stereotactic body radiotherapy (SBRT) for oligometastatic lung tumors from colorectal cancer and other primary cancers in comparison with primary lung cancer. *Radiother. Oncol.* **101**, 255-259.
- Yoshino, H., Kashiwakura, I. (2017) Involvement of reactive oxygen species in ionizing radiation-induced upregulation of cell surface Toll-like receptor 2 and 4 expression in human monocytic cells. *J. Radiat. Res.* **58**, 626-635.
- Zhai, G. G., Malhotra, R., Delaney, M., Latham, D., Nestler, U., Zhang, M., Mukherjee, N., Song, Q., Robe, P., Chakravarti, A. (2006) Radiation enhances the invasive potential of primary glioblastoma cells via activation of the Rho signaling pathway. *J. Neurooncol.* **76**, 227-237.
- Zhang, W. J., Chen, C., Zhou, Z. H., Gao, S. T., Tee, T. J., Yang, L. Q., Xu, Y. Y., Pang, T. H., Xu, X. Y., Sun, Q., Feng, M., Wang, H., Lu, C. L., Wu, G. Z., Wu, S., Guan, W. X., Xu, G. F. (2017) Hypoxia-inducible factor-1 $\alpha$  correlates with tumor-associated macrophages infiltration, influences survival of gastric cancer patients. *J. Cancer* **8**, 1818-1825.
- Zhou, Y. C., Liu, J. Y., Li, J., Zhang, J., Xu, Y. Q., Zhang, H. W., Qiu, L. B., Ding, G. R., Su, X. M., Mei, S., Guo, G. Z. (2011) Ionizing radiation promotes migration and invasion of cancer cells through transforming growth factor- $\beta$ -mediated epithelial-mesenchymal transition. *Int. J. Radiat. Oncol. Biol. Phys.* **81**, 1530-1537.